Electronic Interactions in Dinuclear Platinum and Palladium Ethynylferrocene and Ferrocenylvinylidene Complexes

John H. K. Yip,*[a] Jianguo Wu,[a] Kwok-Yin Wong,*[b] Kam Piu Ho,[b] Lip Lin Koh,[a] and Jagadese J. Vittal[a]

Keywords: Platinum / Palladium / Ferrocene / Alkenes

The complex $[Pd_2(dppm)_2(\mu\text{-}\eta^1{:}\eta^1\text{-}H\text{–}C{=}C\text{–}Fc)Cl_2]$ (**2**) and its vinylidene isomer $[Pd_2(dppm)_2(\mu\text{-}C{=}CH\text{–}Fc)Cl_2]$ (**3**) [dppm = bis(diphenylphosphanyl)methane, Fc = ferrocenyl unit, $CpFeC_5H_4$] have been synthesized and characterized by single-crystal X-ray diffraction. Both **2** and **3** are A-frame structures with long Pd–Pd distances of 3.2055(9) Å (**2**) and 3.1002(2) Å (**3**), respectively, and square-planar metal coordination. The cyclic voltammograms (CV) of the complexes are measured and compared with that of $[Pt_2(dppm)_2(\mu\text{-}\eta^1{:}\eta^1\text{-}H\text{–}C{=}C\text{–}Fc)Cl_2]$ (**1**). The CV of **2** and **3** consist of a nearly reversible Fc-oxidation, an irreversible oxidation and a small reversible couple. The $E_{1/2}$ values (vs. Cp_2Fe^+/Cp_2Fe) of the Fc-groups in complexes **1**–**3** follow the order **2** (–75±8 mV) > **1** (–108±10 mV) > **3** (–124±8 mV). The difference in the $E_{1/2}$ values is explained by the orbital interactions between the acetylene and vinylidene groups with Pt_2 and Pd_2 cores. Our analysis shows that the metal-to-ligand π back-bonding and ligand-to-metal σ-donation have determining effects on the electronic interactions between the dimetallic centers and the bridgehead ligands.

Introduction

Understanding ligand-mediated electronic interactions is pertinent to the design of organometallic-based advanced materials. Special attention has been given to alkynyl (−C≡C−) and polynyl ligands because of the potential applications of their metal complexes in areas such as molecular electronics and photonic materials.[1] While many complexes containing acetylene (R−C≡C−R′)[2] and vinylidene (C=CRR′)[3] have been synthesized, the emphasis of the studies is mostly on the reactivity and structures of the compounds and the knowledge of the electronic interactions in these metal complexes is rather limited. Similar to the alkynyl group, acetylene and vinylidene can participate in π-conjugation with metal centers. However, there are differences between metal−acetylene/−vinylidene bonding and the metal−alkynyl bonding, which is expected to have pronounced effects on the electronic interactions mediated by these ligands. Apparently, a better understanding of the electronic interactions between the metal and the two organic linkages is essential for the exploitation of metal−acetylene and −vinylidene complexes in organometallic materials.

Dinuclear d^9−d^9 $[M_2(L)_2(L')_2]$ complexes (M = Ir^0, Rh^0, Pd^I, Pt^I; L = bridging diphosphane or diarsane, L′ = terminal ligands) are known to react with various groups (X) i.e. CO, acetylene, isocyandide, halides to form the so-called A-frame complexes $[M_2(L)_2(L')_2(\mu\text{-}X)]$ in which the two metal atoms are bridged by the X group in the apical position.[4] The complexes have been studied intensively, mainly for their intriguing structures and reactivity.[4,5] The first comprehensive theoretical study of the bonding of A-frame complexes was given by Hoffmann.[6] The optical spectroscopy and electronic structures of a series of A-frame vinylidene $[Ni_2(dppm)_2(\mu\text{-}C{=}CH_2)X_2]$ (X = Cl, Br, SCN)[7] and the luminescent properties of the distorted A-frame $[Pt_2(\mu\text{-}AuCl)(dppm)_2Cl_2]$ were reported.[8] In view of their structural simplicity and the theoretical underpinning, it is believed that the A-frame acetylene and vinylidene complexes could serve as models in probing the electronic communications mediated by the two unsaturated groups. Our recent study showed that the redox-active ethynylferrocene can be anchored onto an A-frame complex $[Pt_2(dppm)_2(\mu\text{-}\eta^1\text{-}\eta^1\text{-}HC{=}C{-}Fc)Cl_2]$ (**1**) (Fc = ferrocenyl $CpFeC_5H_4$) via the oxidative addition reaction with $[Pt^I{}_2(dppm)_2Cl_2]$.[9] The cyclic voltammogram (CV) of the complex shows a cathodic shift of the reduction potential of the Fc^+/Fc couple, indicating the existence of electronic interactions between the Fc group and the Pt_2 center. In order to further elucidate the electronic interactions between the dimetallic

[a] Department of Chemistry, The National University of Singapore,
10 Kent Ridge Crescent, 119260 Singapore
Fax: (internat.) + 65-67791691
E-mail: chmyiphk@nus.edu.sg
[b] Department of Applied Biology and Chemical Technology, Hong Kong Polytechnic University,
Hunghom, Kowloon, Hong Kong SAR, People's Republic of China

  DOI: 10.1002/ejic.200300595

center and Fc group, we prepared the palladium analog of compound **1**, $[Pd_2(dppm)_2(\mu\text{-}\eta^1\text{-}\eta^1\text{-}HC{=}C{-}Fc)Cl_2]$ (**2**), and its vinylidene isomer $[Pd_2(dppm)_2(\mu\text{-}C{\equiv}CH{-}Fc)Cl_2]$ (**3**) (Scheme 1). Apart from showing the effects of the metal ion and the bridging ligand on the electronic interactions, our results also provide insights into the metal−acetylene and −vinylidene bonding.

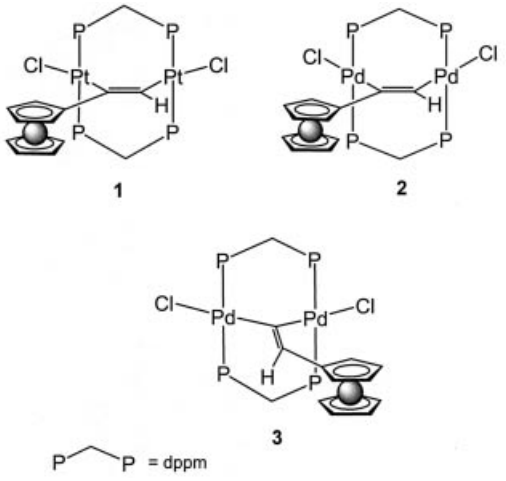

Scheme 1

Results and Discussion

Synthesis and Structures

Like other A-frame dipalladium-acetylene complexes,[10] $[Pd_2(dppm)_2(\mu_2\text{-}\eta^1{:}\eta^1\text{-}H{-}C{\equiv}C{-}Fc)Cl_2]$ (**2**) was synthesized from a reaction between $[Pd_2(dppm)_2Cl_2]$ and ethynylferrocene. The synthesis of the vinylidene complex $[Pd_2(dppm)_2(\mu\text{-}C{\equiv}CH{-}Fc)Cl_2]$ (**3**) is different from the conventional method which involves acid catalyzed isomerization of the dipalladium-acetylene complex[11] or reaction of $[Pd_2(dppm)_2Cl_2]$ with diiodoalkenes.[12] Refluxing a methanol solution of compound **2** with HBF_4 failed to transform complex 2 into its vinylidene isomer. We discovered that the vinylidene complex can be synthesized in moderate yield by the reaction between $[Pd_2(dppm)_2Cl_2]$ and ferrocenylacetylide ($Fc{-}C{\equiv}C^-$), which was generated from the deprotonation of $Fc{-}C{\equiv}C{-}H$ by NaOMe generated in situ. The formation of complex **3** may involve the reduction of $Fc{-}C{\equiv}C^-$ by the Pd−Pd bond (Scheme 2).

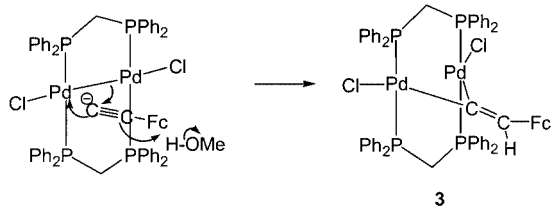

Scheme 2

The Pt-vinylidene complex, $[Pt_2(dppm)_2(\mu\text{-}C{=}CHFc)Cl_2]$, cannot by synthesized by this method or acid-catalyzed isomerization of compound **1**. As reported earlier, the reaction between $[Pt_2(dppm)_2Cl_2]$ and $FcC{\equiv}C^-$ led to the formation of $[Pt_2(dppm)_2(C{\equiv}C{-}Fc)_2]$.[13]

The complex **2** is isostructural to its Pt analog $[Pt_2(dppm)_2(\mu_2\text{-}\eta^1{:}\eta^1\text{-}H{-}C{\equiv}C{-}Fc)Cl_2]$, the structure of which was recently reported by us.[9] The X-ray crystal structure of compound **2** shows two nearly square-planar Pd ions bridged by two *trans* oriented dppm groups and one ethynylferrocene (Figure 1 and Table 1). Two chloride ions are coordinated *trans* to the two acetylene carbon atoms [C(1)−Pd(1)−Cl(1) = 170.1(3)°, C(2)−Pd(2)−Cl(2) 171.4(3)°]. As observed in many other dppm-bridged dinuclear compounds, the $Pd_2(P{-}C{-}P)_2$ metallocycle in **2** adopts a boat conformation. The Pd−P and Pd−Cl bond lengths are normal.[10,11,12] The Pd−C bond lengths, which are slightly different [Pd(1)−C(1) = 2.010(1) Å and Pd(2)−C(2) = 2.038(1) Å], are similar to the ones found in similar complexes such as $[Pd_2(dppm)_2(\mu_2\text{-}\eta^1{:}\eta^1\text{-}F_3C{-}C{=}C{-}CF_3)Cl_2]$ [Pd−C = 1.994(12) and 2.014(12) Å].[10] The long Pd−Pd distance of 3.2055(9) Å indicates the absence of a metal−metal bond; in other words, the two d^9 Pd^I ions in $[Pd_2(dppm)_2Cl_2]$ are formally oxidized to d^8 Pd^{II} ions in **2**. The distorted square-planar coordination geometry of the Pd ions is characteristic of d^8 metals. Accordingly the bridging ligand should be regarded as a dianionic ethylene $(H{-}C{=}C{-}Fc)^{2-}$, as suggested by the theoretical study.[6] In line with the assignment of the bridging acetylene as a dianionic ethylene $(H{-}C{=}C{-}Fc)^{2-}$ is the acetylene C(1)−C(2) bond length [1.309(14) Å], which is significantly longer than the averaged C≡C bond length (1.19 Å) but falls into the range of an average C=C bond. In addition, the angles between the bridging acetylene and the Pd atoms [Pd(1)−C(1)−C(2) = 117.2(8)° and Pd(2)−C(2)−C(1) = 118.4(8)°] are close to 120° expected for an sp^2 carbon. Similar bond angles and acetylene C−C distances are found in complex **1** [Pt−C−C = 120.4(7)° and 116.8(7)°, C−C = 1.293(1) Å]. The angles θ, which measure the deviation of

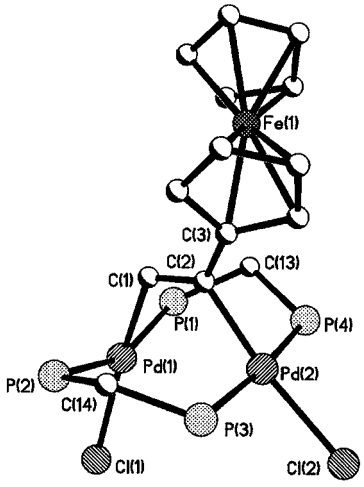

Figure 1. Molecular structure of compound **2**·CH_2Cl_2. All the H-atoms and solvent molecules are omitted for clarity

the Pd−Cl bonds from the Pd−Pd vector (Scheme 3), are 52.74(9)° and 69.83(9)°. Similar angles θ [53.30(9)°, 69.44(9)°] were observed in the complex **1**. The $^{31}P\{^{1}H\}$ NMR spectrum of the complex is second-order showing two multiplets (AA′BB′)[10] at δ = 4.80 and 10.58.

Table 1. Selected bond length [Å] and angles [deg] for **2**·CH_2Cl_2

Pd(1)−C(1)	2.010(1)	Pd(2)−C(2)	2.038(1)
Pd(1)−Cl(1)	2.396(3)	Pd(2)−Cl(2)	2.407(2)
Pd(1)−Pd(2)	3.2055(9)	C(2)−C(3)	1.452(1)
C(1)−C(2)	1.309(1)	P(3)−Pd(2)−P(4)	173.34(9)
P(1)−Pd(1)−P(2)	157.29(9)	P(2)−Pd(1)−Cl(1)	95.72(1)
P(1)−Pd(1)−Cl(1)	105.08(1)	P(4)−Pd(2)−Cl(2)	91.66(9)
P(3)−Pd(2)−Cl(2)	171.4(3)	C(2)−Pd(2)−Cl(2)	171.4(3)
C(1)−Pd(1)−Cl(1)	170.1(3)	C(1)−C(2)−Pd(2)	118.4(8)
C(2)−C(1)−Pd(1)	117.2(8)		
C(1)−C(2)−C(3)	126.2(9)		

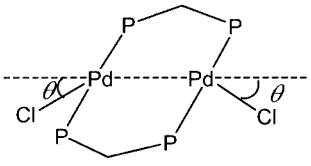

Scheme 3

The X-ray crystal structure $[Pd_2(dppm)_2(\mu\text{-}C{\equiv}CH{-}Fc)Cl_2]$ (**3**) (Figure 2 and Table 2) features a $[Pd_2(dppm)_2Cl_2]$ core similar to that of complex **2**. The two metal ions are bridged by the α-carbon atom of the ferrocenylvinylidene. The Fc group is disordered over two positions (50% occupancy for each position) which are symmetric with respect to the two Pd atoms. The α-carbon atom is equidistant from the two metal ions [Pd(1)−C(2) = 19.18(11) Å]. Although the Pd−Pd distance [3.1002(17) Å] is shorter than those reported in other A-frame Pd_2−vinylidene complexes, it is still too long to assign any formal bonding between the metal ions; accordingly, the Pd and the bridging ligand should be formulated as Pd^{II} and $Fc{-}CH{=}C^{2-}$, respectively. The bridging angle, Pd(1)−C(1)−Pd(1A), 107.8(9)°, is smaller than the 120° of an sp^2 carbon. This is by no means unique to the present complex, as a similar bridging angle is found in related compounds, i.e. $[Pd_2(dppm)_2(\mu\text{-}C{=}CH_2)Cl_2]$ [Pd−C−Pd = 109.2(8)°]. Due to their high thermal parameters, the distance between the two vinylidene carbon atoms C(2)−C(3) cannot be determined accurately. The angle θ, 38.16(2)°, is smaller than that in complex **2**. No ν(C≡C) vibration is observed in the IR spectrum of **3**. The $^{31}P\{^{1}H\}$ NMR spectrum is in accordance with the molecular structure of the complex as it shows two second-order multiplets centered at δ 13.5 which display a splitting pattern ascribable to the AA′BB′ system.[10]

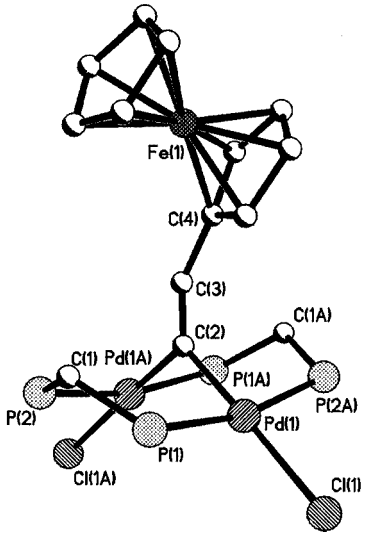

Figure 2. Molecular structure of compound **3**. All the H-atoms and solvent molecules are omitted for clarity

Table 2. Selected bond length [Å] and angles [deg] for **3**

Pd(1)−C(2)	1.918(1)	Pd(1A)−C(2)	1.918(11)
Pd(1)−Cl(1)	2.408(4)	Pd(1)−Pd(1A)	3.1002(2)
C(2)−C(3)	1.20(3)	C(3)−C(4)	1.44(3)
P(1)−Pd(1)−P(2A)	166.89(2)	P(2A)−Pd(1)−C(2)	84.12(11)
C(2)−Pd(1)−P(1)	86.78(8)	C(2)−Pd(1)−Cl(1)	177.9(5)
P(2A)−Pd(1)−Cl(1)	96.01(2)	P(1)−Pd(1)−Cl(1)	93.43(12)
C(3)−C(2)−Pd(1A)	126.1(4)	P(1)−Pd(1)−Pd(1A)	141.84(2)
C(4)−C(2)−C(3)	152.7(6)	Pd(1A)−C(2)−Pd(1)	107.8(9)

Electrochemistry of the Complexes

The electrochemical data of the complexes **1**−**3** are summarized in Table 3. Our previous study showed that, at room temperature, the cyclic voltammogram (CV) of **1** shows a reversible Fc^+/Fc-couple (ΔE_p = 60 mV, i_c/i_a = 1) at −108±10 mV vs. Cp_2Fe^+/Cp_2Fe.[9] There is an irreversible oxidation at 583±10 mV attributable to the oxidation of the Pt metal center. The corresponding Pt reduction occurs at 343±10 mV. No reduction wave was observed when the initial scan direction was made towards the cathodic side.

The CV of **2** measured in CH_2Cl_2 at room temperature (Figure 3) displays a reversible couple at $E_{1/2}$ = −75±8 mV (vs. Cp_2Fe^+/Cp_2Fe, $i_{pc}/i_{pa} \approx 1$, ΔE_p = 77 mV), an irreversible oxidation peak II at +487±8 mV, and a reversible couple III at $E_{1/2}$ = +833±8 mV ($i_{pc}/i_{pa} \approx 1$). Couple I at $E_{1/2}$ = −75±8 mV is attributable to the one-electron oxidation of the Fc group as its reduction potential is close to the Fc^+/Fc-couple of **1**. The peak-to-peak splitting (ΔE_p) of 77 mV is slightly larger than the 60 mV expected for a reversible one-electron couple. This is likely to be caused by the resistance of the dichloromethane electrolyte and the liquid junction potential between the reference electrode and the electrolyte. The reversible oxidation of the Fc group is followed by an irreversible oxidation wave II at +487±8 mV. The size of this irreversible oxidation wave is close to that of the Fc^+/Fc-couple, indicating that it too is a one-electron process. Reversing the voltammetric scan at 550 mV did not

Table 3. Electrochemical data of compounds **1**, **2**, and **3**[a]

Complex[a]	Fc^+/Fc-couple I[b] $E_{1/2}$	Irreversible oxidation peak II[b] (reduction peak)	Reversible couple III[b] $E_{1/2}$
1	−108±10	+583±10 (343±10)	
2	−75±8	+487±8 (+330±8)	+833±8
3	−124±8	+679±8 (+623±8)	+969±8

[a] Measured in CH_2Cl_2 (0.1 M nBu_4NPF_6), working electrode: glassy carbon electrode (0.07 cm^2), reference electrode: $Ag/AgNO_3$ (0.1 M in CH_3CN), counter electrode: platinum wire. [b] mV vs. Cp_2Fe^+/Cp_2Fe.

result in the observation of the corresponding reduction wave for this oxidation. A small reduction peak, however, was observed at +311±8 mV in the reverse scan. This indicates that **2**, once oxidized at this potential, rapidly undergoes an irreversible 'chemical reaction'. Theoretical calculations on the isoelectronic and isostructural A-frame Rh^I_2(μ-acetylene) showed that the HOMO of the complex is mostly metal-based.[6] This suggests that the oxidation process at 487±8 mV could correspond to the one-electron oxidation of $Pd^{II}Pd^{II}$ to $Pd^{II}Pd^{III}$. Since Pd^{III} and Pd^{II} ions prefer different coordination geometries, the oxidation brings about drastic structural changes, which could account for the 'chemical reaction' following the electron transfer. The small reduction wave at 311±8 mV could be due to the product after the structural rearrangement has occurred. The irreversible oxidation at 487±8 mV is followed by a smaller but reversible couple III at $E_{1/2}$ = +833±8 mV. The smaller size of this couple compared to the Fc^+/Fc-couple is consistent with the structural rearrangement of the complex preceding the electron transfer. Tentatively the couple is assigned to the oxidation of $Pd^{III}Pd^{II}$ to $Pd^{III}Pd^{III}$.

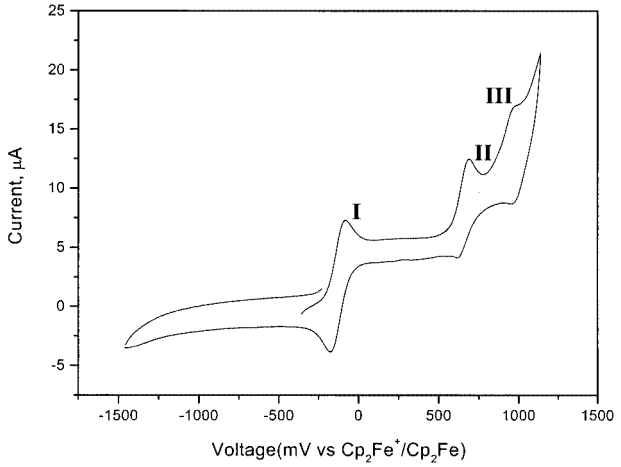

Figure 3. CV of **2** measured in CH_2Cl_2 (0.1 M nBu_4NPF_6), working electrode: glassy carbon electrode (0.07 cm^2), reference electrode: $Ag/AgNO_3$ (0.1 M in CH_3CN), counter electrode: platinum wire, concentration of complex = 1.2 mM, scan rate = 10 mV/s

Similar to compound **2**, the CV of the vinylidene complex **3** (Figure 4) exhibits a reversible couple I at $E_{1/2}$ = −124 ± 8 mV ($i_{p,c}/i_{p,a} \approx 1$; ΔE_p = 74 mV), an irreversible oxidation peak II at +679±8 mV and a smaller reversible couple at $E_{1/2}$ = +969±8 mV ($i_{p,c}/i_{p,a} \approx 1$). The reversible couple I $E_{1/2}$ = −124 mV is assigned to the Fc^+/Fc-couple. The size of the irreversible wave II at +679±8 mV is similar to that of the Fc^+/Fc-couple and is therefore assigned to the one-electron oxidation of Pd^{II} Pd^{II} to $Pd^{II}Pd^{III}$. A small reduction peak appeared at +623±8 mV, which is attributed to reduction of the rearranged product after the oxidation process has occurred. The smaller reversible couple III at +969±8 mV could be due to the oxidation of $Pd^{II}Pd^{III}$ to $Pd^{III}Pd^{III}$.

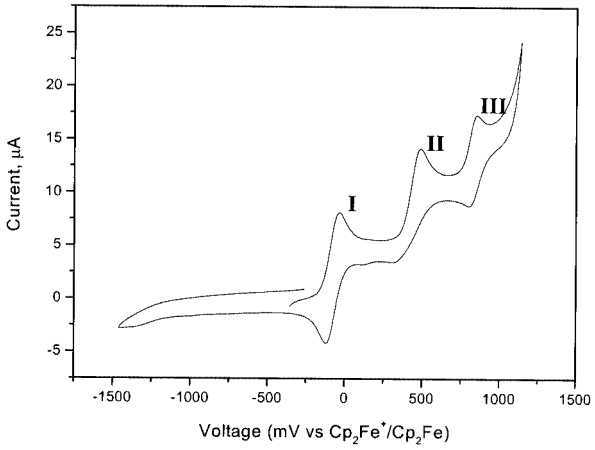

Figure 4. CV of **3** measured in: CH_2Cl_2 (0.1 M nBu_4NPF_6), working electrode: glassy carbon electrode (0.07 cm^2), reference electrode: $Ag/AgNO_3$ (0.1 M in CH_3CN), counter electrode: platinum wire, concentration of complex = 1.2 mM, scan rate = 10 mV/s

Electronic Interactions

A common electrochemical feature of the complexes is the low $E_{1/2}$ of their Fc^+/Fc-couples in comparison with the reported $E_{1/2}$ of ethynylferrocene (Fc^+−C≡CH/Fc−C≡CH = +254 mV vs. Cp_2Fe^+/Cp_2Fe).[14] In other words, the Fc groups in the three dinuclear complexes are more reducing or electron-rich than the one in the uncomplexed Fc−C≡C−H. This is consistent with the formal assignment of the bridgehead ligands as the dianionic $(H-C=C-Fc)^{2-}$ and $Fc-CH=C^{2-}$ species. Since the Fc groups in these complexes are connected to the acetylene and vinylidene groups via σ- and π-bonds, transfer of electron density from the dimetallic cores onto the linkage would lower the potential of the Fc^+/Fc-couple via π-conjugation and an inductive effect.

Comparing the $E_{1/2}$ of the Fc^+/Fc-couples of the isostructural compounds **1** and **2** shows that the Fc group in the Pd_2 complex (−75±8 mV) is less reducing than the one in the Pt_2 complex (−108±10 mV). The interactions between the dianionic $(H-C{\equiv}C-Fc)^{2-}$ and the dinuclear M_2 centers (M = Pd^{II} and Pt^{II}) consist of σ- and π-donations from the ligand π-orbitals and the metal-to-ligand π back-bonding (Scheme 4). The bending of the $(H-C{\equiv}C-Fc)^{2-}$ unit lifts the degeneracy of the π- and π*-orbitals, with the energy in the order: $\pi_x^2 < \pi_z^2 < \pi^*_z{}^2 < \pi^*_x$ (*x* axis is parallel to the meridian of the complex).[6] In addition, the π_z- and π_z*-orbitals are hybridized with the 2s-orbital. The ligand(π_x)-to-metal π-donation is secondary as there is no low-lying accepting orbital in the metals to interact with the deep-seated π_x-orbital. In first-order approximation, the ligand-to-metal σ-donation involves, primarily, interactions between the filled bonding π_z- and antibonding π_z*-orbitals of $(H-C{\equiv}C-Fc)^{2-}$ and the empty dσ- and dσ*-orbitals, respectively. The latter orbitals arise from the bonding and antibonding combinations of the two $nd_{x^2-y^2}$-orbitals (*n* = 4 for M = Pd and 5 for M = Pt). While electron density drifts from $(H-C{\equiv}C-Fc)^{2-}$ to the M_2 core as a result of σ-donation, the metal-to-ligand π back-bonding, which involves the nd_{xy}-orbitals of M_2 and the π_x*-orbital of $(H-C{\equiv}C-Fc)^{2-}$, transfers electron density from the metal to the $(H-C{\equiv}C-Fc)^{2-}$ unit. The importance of the ligand-to-metal σ-donation in the interactions is obvious but the significance of the metal-to-ligand π back-bonding in the electronic interactions is rather uncertain. In view of the general conception that third row transition metals form stronger π back-bonding than their second row congeners, one would expect the $Pt_2 \rightarrow (H-C{\equiv}C-Fc)^{2-}$ π back-bonding to be stronger than the $Pd_2 \rightarrow (H-C{\equiv}C-Fc)^{2-}$ π back-bonding. This is consistent with the $E_{1/2}$ values of the Fc^+/Fc-couples in **1** and **2**.

The $E_{1/2}$ of the Fc^+/Fc-couple of the vinylidene complex (−124±8 mV) is lower than the corresponding $E_{1/2}$ of its acetylene isomer **2** (−75±8 mV). The Fc group of **3** is even more reducing than that of **1**, which suggests the metal-to-ligand π back-bonding is not the main cause for the low reduction potential. We believe that this difference in the reduction potentials could be interpreted as a weaker $Fc-CH{=}C^{2-} \rightarrow Pd_2$ σ-donation in complex **3**. Notably, the peak potential of the irreversible metal oxidation of complex **2** (+487±8 mV) is lower than that of complex **3** (+679±8 mV), suggesting that Pd_2 in **2** is more electron-rich than that in **3**. This is consistent with the argument that the $(H-C{\equiv}C-Fc)^{2-} \rightarrow Pd_2$ donation is stronger than the $Fc-CH{=}C^{2-} \rightarrow Pd_2$ donation. The σ-bonding in complex **3** involves the interactions between (i) the filled antibonding π*-orbital (vinylidene) and the dσ*-orbital (Pd_2) and (ii) an admixture of 2s- and $2p_y$-orbitals (vinylidene) and the dσ-orbital (Pd_2) (Scheme 5). The splitting of the dσ- and dσ*-orbitals would be increased by a better overlap of the two $d_{x^2-y^2}$-orbitals.[6] This can be achieved by shortening the Pd−Pd distance or reducing the angle θ. Comparing the structures of the two isomers shows that the Pd−Pd distance [3.1002(17) Å] and the angle θ [38.16(2)°] are shorter and smaller than the ones in complex **2** [Pd−Pd = 3.2055(9) Å; θ = 52.74(9)°, 69.83(9)°]. These structural features suggest that the dσ*-orbital in complex **3** is more destabilized than the one in complex **2**. The larger energy separation between the π_y*- and dσ*-orbitals weaken the σ-donation. On the other hand, one would expect the 2s/2p−dσ interaction to be enhanced as the dσ-orbital is now more stabilized. Nonetheless, the $E_{1/2}$ of the Fc group should be determined mainly by the π_y*−dσ* interaction since the π_y*-orbital is higher in energy than it is in π-conjugation with the Cp-ring of the Fc group. Another possibility for the poorer σ-donation in complex **3** is the relatively in-

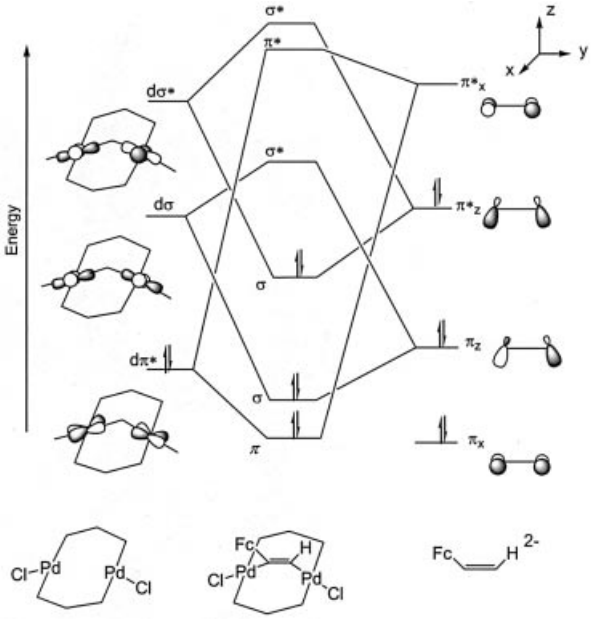

Scheme 4

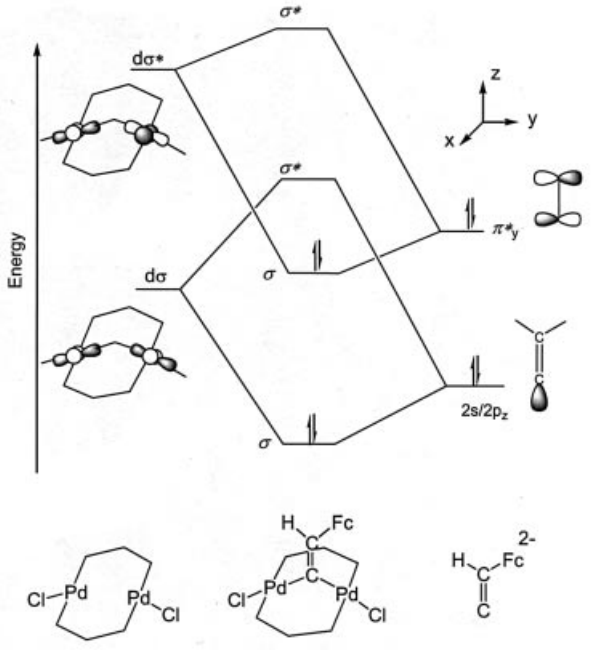

Scheme 5

sufficient overlap between the apical carbon sp^2-hybridized orbital and the metal orbitals; suggested by the fact that the bridging angle Pd−C−Pd [107.8(9)°] is smaller than 120°. On the other hand, the orbital overlap between $(H-C{=}C-Fc)^{2-}$ and Pd_2 in complex **2** is better as the Pd(1)−C(1)−C(2) and Pd(2)−C(2)−C(1) angles [117.2(8)° and 118.4(8)°] are close to the ideal angle of an sp^2-hybridized carbon atom. This poor σ-donation would retain more electron density in the vinylidene from which the inductive effect would be transmitted via the σ-bonds to the ferrocenyl group, leading to a lower Fc^+/Fc potential as observed.

Concluding Remarks

In summary, our work demonstrated the presence of electronic interactions between the ferrocenyl group and the metal centers in the complexes $[Pd_2(dppm)_2(\mu\text{-}\eta^1{:}\eta^1\text{-}H-C{=}C-Fc)Cl_2]$ and $[Pd_2(dppm)_2(\mu\text{-}C{=}CH-Fc)Cl_2]$. Comparing the $E_{1/2}$ of the Fc^+/Fc-couples of $[Pd_2(dppm)_2(\mu\text{-}\eta^1{:}\eta^1\text{-}H-C{=}C-Fc)Cl_2]$ and its Pt-analog shows that the Pt has stronger metal-to-ligand π backbonding than the Pd. It is rather unexpected that the ligand-to-metal σ-donation in the Pd_2−μ-vinylidene complex is weaker than the one in the acetylene isomer. This is attributed to the destabilization of the dσ*-orbital and the poor orbital overlap between the bridging vinylidene and the metal ions.

Experimental Section

General Methods: All syntheses were carried out using standard Schlenk techniques. All solvents used in syntheses and electrochemical measurements were purified according to the literature methods. The supporting electrolyte $n\text{Bu}_4\text{NPF}_6$ (TBAH) obtained from Aldrich was recrystallized from ethanol and dried at 100 °C for 24 h before being used. Ethynylferrocene[15] and $[Pd_2(dppm)_2Cl_2]$[16] were prepared according to reported procedures. Dichloromethane used for the voltammetric measurements was distilled over P_2O_5.

Physical Measurements: NMR spectra were recorded at 25 °C on a Bruker ACF 300 spectrometer. Elemental analyses of the complexes were carried out in the microanalysis laboratory in the department of chemistry, the National University of Singapore. Solution infrared spectra of the complexes were recorded on a Bio-Rad TFS 156 spectrometer. A Bioanalytical Systems (BAS) model 100 W electrochemical analyzer was used in all electrochemical measurements. $n\text{Bu}_4\text{NPF}_6$ (0.1 M) was used as the supporting electrolyte unless otherwise stated. Cyclic voltammetry was performed in a conventional two-compartment electrochemical cell. The platinum disc working electrode (area 0.02 cm^2) was treated by polishing it with 0.05 μm alumina using a microcloth and then sonicated for 5 minutes in deionized water followed by rinsing with the solvent used in the electrochemical studies. An $Ag/AgNO_3$ (0.1 M in CH_3CN) electrode was used as reference electrode. The potential of the $Ag/AgNO_3$ reference electrode was calibrated against the $Cp_2Fe^{+/0}$ couple before and after each set of experiments to ensure the accuracy of the potential measured;[17] the $E_{1/2}$ of $Cp_2Fe^{+/0}$ was found to be 0.06±0.01 V vs. the $Ag/AgNO_3$ reference. The $E_{1/2}$ values are the average of the cathodic and anodic peak potentials for the oxidative and reductive waves of reversible couples.[18]

Synthesis of $[Pd_2(dppm)_2(\mu\text{-}\eta^1{:}\eta^1\text{-}HC{=}C-Fc)Cl_2]\cdot CH_2Cl_2$ ($2\cdot CH_2Cl_2$): A methanol suspension of $[Pd_2(dppm)_2Cl_2]$ (0.3 g, 0.29 mmol) and ethynylferrocene (0.06 g, 0.29 mmol) was stirred at room temperature for 24 h and the orange precipitate that formed was filtered. The solid was dissolved in dichloromethane and filtered. Excess diethyl ether was added to the filtrate to precipitate the product as an orange solid. The product was purified by diffusing diethyl ether into a dichloromethane solution. Yield 59%. $C_{63}H_{56}Cl_4FeP_4Pd_2$: calcd. C 56.11, H 4.16; found C 56.00, H 4.12 (%). ^{1}H NMR (300 MHz, CD_2Cl_2, δ/ppm): 5.42 (m, 1 H, H−C=), 3.06 (m, 2 H, PCH_2P), 3.41 (s, 5 H, C_5H_5), 3.41 (s, 4 H, C_5H_4), 3.25 (m, 2 H, PCH_2P), 6.94−7.98 (m, 40 H, Ph). $^{31}P\{^1H\}$ NMR (300 MHz, CD_2Cl_2, δ/ppm): 4.80 (m, 2 P), 10.58 (m, 2 P).

Synthesis of $[Pd_2(dppm)_2(\mu\text{-}C{\equiv}CH-Fc)Cl_2]$ (3): Sodium (0.02 g, 0.855 mmol) was added to a methanol solution (10 mL) of ethynylferrocene (0.18 g, 0.86 mmol). After 20 min of stirring hexane (60 mL) was introduced, followed by the addition of $[Pd_2(dppm)_2Cl_2]$ (0.30 g, 0.29 mmol). The mixture was stirred at room temperature for 12 h and then filtered. The solid was dissolved in dichloromethane and filtered. Excess diethyl ether was added to the filtrate to precipitate the product as an orange solid. The product was purified by diffusing diethyl ether into a dichloromethane solution. Yield 45%. $C_{62}H_{54}Cl_2FeP_4Pd_2$: calcd. C 58.93, H 4.28; found C 58.46, H 4.12 (%). ^{1}H NMR (300 MHz, CD_2Cl_2, δ/ppm): 5.56 (m, 1 H, H−C=C), 2.60 (m, 2 H, PCH_2P), 3.67 (s, 5 H, C_5H_5), 4.02 (s, 4 H, C_5H_4), 3.10 (m, 2 H, PCH_2P), 6.95−7.92 (m, 40 H, Ph). $^{31}P\{^1H\}$ NMR (300 MHz, CD_2Cl_2, δ/ppm): 12.7−14.5 (m).

X-ray Crystallography: The diffraction experiments were carried out on a Bruker AXS SMART CCD 3-circle diffractometer at T = 223 K, 2θ−ω scan with a sealed tube using graphite-monochromated Mo-K_α radiation (λ = 0.71073 Å). The following software was used: SMART[19] for collecting frames of data, indexing reflection and determination of lattice parameters; SAINT[19] for integration of intensity of reflections and scaling; SADABS[20] for empirical absorption correction; and SHELXTL[21] for space group determination, structure solution and least-squares refinements on $|F|^2$. The crystals were mounted at the end of glass fibers. Anisotropic thermal parameters were refined for the non-hydrogen atoms. The hydrogen atoms were placed in their ideal positions. A brief summary of crystal data and experimental details are given in Table 4. Crystallographic data for (i) **$[Pd_2(dppm)_2(\mu\text{-}\eta^1{:}\eta^1\text{-}HC{=}CFc)Cl_2]\cdot CH_2Cl_2$** ($2\cdot CH_2Cl_2$): of the 16441 reflections collected, 10837 were independent (R_{int} = 0.0466). Index range: $-15 \le h \le 17$, $-17 \le k \le 16$, $-21 \le l \le 19$. Refinement of F^2 converged with R_1 = 0.0982 for $I > 2\sigma(I)$ and wR_2 = 0.2672. The residual electron density is 3.142 and −2.392 e·Å^{-3}, (ii) **$[Pd_2(dppm)_2(\mu\text{-}C{=}CH-Fc)Cl_2]$ (3)**: of the 25934 reflections collected, 5298 were independent (R_{int} = 0.0747). Index range: $-19 \le h \le 18$, $-18 \le k \le 18$, $-24 \le l \le 15$. Refinement of F^2 converged with R_1 = 0.0611 for $I > 2\sigma(I)$ and wR_2 = 0.1648. The residual electron density is 0.394 and −0.239 e·Å^{-3}. The ferrocenyl unit is disordered over two positions with 50% occupancy. One of the phenyl groups is disordered and is modeled with two orientations, each with 50% occupancy.

CCDC-217655 (for **2**), and -217656 (for **3**) contain the supplementary crystallographic data for this paper. These data can be obtained free of charge at www.ccdc.cam.ac.uk/conts/retrieving.html [or from the Cambridge Crystallographic Data Centre, 12, Union

Table 4. Crystal data and structure refinements for **2**·CH_2Cl_2 and **3**

	2·CH_2Cl_2	**3**
Formula	$C_{63}H_{56}Cl_4FeP_4Pd_2$	$C_{62}H_{54}Cl_2FeP_4Pd_2$
Molecular mass	1347.41	1262.48
Crystal system	triclinic	trigonal
Space group	$P\bar{1}$	$P3(1)21$
Z	2	3
Crystal size [mm^3]	0.6 × 0.6 × 0.56	0.56 × 0.46 × 0.16
Lattice parameters [Å]	a = 14.3059(2), b = 14.4442(2), c = 17.8761(3)	a = 16.017(4), b = 16.017(4), c = 20.353(7)
[deg]	α = 80.544(1), β = 71.517(1), γ = 67.986(1)	α = 90(1), β = 90(1), γ = 120(1)
V [A^3]	3236.29(8)	4522(2)
Density (calcd.) [$g \cdot cm^{-3}$]	1.383	1.391
Abs. coeff. [mm^{-1}]	1.070	1.058
$F(000)$	1360	1914
No. of parameters varied	670	335
Final R indices[a]	$R1$ = 0.0982. $wR2$ = 0.2672	$R1$ = 0.0611. $wR2$ = 0.1648
Goodness of fit[b]	1.122	0.904

[a] $R1 = (||F_o| - |F_c||)/(|F_o|)$; $wR2 = [w(F_o^2 - F_c^2)/w(F_o^4)]^{1/2}$. [b] GOF = $[w(F_o^2 - F_c^2)^2/(n - p)]^{1/2}$.

Road, Cambridge CB2 1EZ, UK; Fax: (internat.) +44-1223/336-033; E-mail: deposit@ccdc.cam.ac.uk].

Acknowledgments

J. H. K. Y. thanks The National University of Singapore for financial supports. K.Y.W. acknowledges the support from the Hong Kong Polytechnic University. We are grateful to Ms Tan Geok Kheng (NUS) for her assistance with the X-ray crystal structure determination.

[1] [1a] I. R. Whittal, A. M. McDonagh, M. G. Humphrey, *Adv. Organomet. Chem.* **1998**, *42*, 291. [1b] J. Manna, K. J. John, M. D. Hopkins, *Adv. Organomet. Chem.* **1995**, *38*, 79. [1c] S. R. Marder, in: *Inorganic Materials* (Eds.: D. W. Bruce, D. O'Hare), Wiley, Chichester, **1996**, p. 121. [1d] N. J. Long, C. K. Williams, *Angew. Chem. Int. Ed.* **2003**, *42*, 2586. [1e] C. R. Horn, J. A. Gladysz, *Eur. J. Inorg. Chem.* **2003**, 2211.

[2] [2a] P. K. Baker, *Adv. Organomet. Chem.* **1996**, *40*, 45. [2b] R. D. Adams, B. Qu, *Organometallics* **2000**, *19*, 2411. [2c] P. J. Low, R. Rousseau, P. Lam, K. A. Udachin, G. D. Enright, J. S. Tse, D. D. M. Wayner, A. J. Carty, *Organometallics* **1999**, *18*, 3885.

[3] [3a] C. Bruneau, P. H. Dixneuf, *Acc. Chem. Res.* **1999**, *32*, 311. [3b] M. Knorr, G. R. Schmitt, M. M. Kubicki, E. Vigier, *Eur. J. Inorg. Chem.* **2003**, 514. [3c] E. Bustelo, J. J. Carbo, A. Lledos, K. Mereiter, M. C. Puerta, P. Valerga, *J. Am. Chem. Soc.* **2003**, *125*, 3311. [3d] S. Hartmann S, R. F. Winter, B. M. Brunner, B. Sarkar, A. Knodler, I. Hartenbach, *Eur. J. Inorg. Chem.* **2003**, 876. [3e] K. Ilg, H. Werner, *Angew. Chem. Int. Ed.* **2000**, *39*, 1632.

[4] [4a] R. J. Puddephatt, *Chem. Soc. Rev.* **1983**, *12*, 99. [4b] C. F. J. Barnard, M. J. H. Russeh, in: *Comprehensive Coordination Chemistry* (Ed.: G. Wilkinson), vol. 5. Pergamon Press, Oxford, **1987**, chapter 51, p. 1099−1130. [4c]G. K. Anderson, *Adv. Organomet. Chem.* **1993**, *35*, 1.

[5] [5a] M. P. Brown, R. J. Puddephatt, M. Rashidi, K. R. Seddon, *J. Chem. Soc., Dalton Trans.* **1978**, 1540. [5b] A. L. Balch, L. S. Benner, M. M. Olmstead, *Inorg. Chem.* **1979**, *18*, 2996. [5c] M. C. Grossel, R. P. Moulding, K. R. Seddon, *Inorg. Chim. Acta* **1983**, *64*, L275. [5d] K. R. Grundy, K. N. Robertson, *Organometalics* **1983**, *2*, 1736.

[6] D. M. Hoffman, R. Hoffmann, *Inorg. Chem.* **1981**, *20*, 3543.

[7] J. D. Heise, J. J. Nash, P. E. Fanwick, C. P. Kubiak, *Organometallics* **1996**, 15, 1690.

[8] D. V. Toronto, A. L. Balch, D. S. Tinti, *Inorg. Chem.* **1994**, *33*, 2507.

[9] J. H. K. Yip, J. Wu, K.-Y. Wong, K.-W. Yeung, J. J. Vittal, *Organometallics* **2002**, *21*, 1612.

[10] C.-L. Lee, C. T. Hunt, A. L. Balch, *Inorg. Chem.* **1981**, *20*, 2498.

[11] [11a] J. A. Davis, K. Kirschbaum, C. Kluwe, *Organometallics* **1994**, *13*, 3664. [11b] C. Kluwe, J. Muller, J. A. Davis, *J. Organomet. Chem.* **1996**, *526*, 385. [11c] C. Kluew, J. A. Davis, *Organometallics* **1995**, *14*, 4257.

[12] J. A. Davis, A. A. Pinkerton, R. Syed, M. Vilmer, *J. Chem. Soc., Chem. Com.* **1988**, 47.

[13] J. H. K. Yip, J. Wu, K.-Y. Wong, K. P. Ho, C. S.-N. Pun, J. J. Vittal, *Organometallics* **2002**, *21*, 5292−5233.

[14] H. Nock, H. Schottenberger, *J. Org. Chem.* **1993**, *58*, 7048.

[15] J.-G. Rodriquez, A. Oñate, R. M. Martin-Villami, I. Fonseca, *J. Organomet. Chem.* **1996**, *513*, 71.

[16] P. G. Pringle, B. L. Shaw, *J. Chem. Soc., Dalton Trans.* **1983**, 889.

[17] G. Gritzner, J. Kúta, *Pure and Appl. Chem.* **1982**, *54*, 1527.

[18] R. R. Gagné, C. A. Koval, G. C. Lisensky, *Inorg. Chem.* **1980**, *19*, 2855.

[19] *SMART & SAINT Software Reference Manuals*, Version 4.0, Siemens Energy & Automation, Inc., Analytical Instrumentation, Madison, Wisconsin, USA, **1996**.

[20] G. M. Sheldrick, *SADABS a software for empirical absorption correction*, University of Gottingen, Gottingen, Germany, **1996**.

[21] *SHELXTL Reference Manual*, Version 5.03, Siemens Energy & Automation, Inc., Analytical Instrumentation, Madison, Wisconsin, USA, **1996**.

Received August 25, 2003
Early View Article
Published Online January 28, 2004

